SIGNAL TO NOISE RATIO ESTIMATION IN PASSIVE CORRELATION BASED IMAGING

Adrien Semin

(joint with Josselin Garnier, George Papanicolaou and Chrysoula Tsogka)

Institute of Applied and Computational Mathematics, Heraklion, Greece
Foundation Of Research and Technology - Hellas
asemin@iacm.forth.gr

ABSTRACT

We consider here the problem of imaging using passive incoherent recordings due to ambient noise sources. The first step towards imaging in this configuration is the computation of the cross-correlations of the recorded signals. These cross-correlations are computed between pairs of sensors (receivers) and they contain very important information about the background medium. Indeed, it was shown both experimentally [1] and theoretically [2] that the Green's function between two sensors can be retrieved from the cross-correlation of passive incoherent recordings at these sensors. Here, we propose to employ these cross-correlations for imaging reflectors using a travel time migration method. The signal to noise ratio analysis of the proposed method is carried out.

1. INTRODUCTION

It is well known [3, 5, 6, 7] that cross-correlations of signals recorded at passive sensors generated by ambient noise sources can be used for the estimation of the Green's function in-between the sensors. Although the theory states that the full Green's function can be obtained [8, 9], in practice for imaging applications [3, 5], or for background velocity estimation [10], extracting the travel time between the two sensors is enough.

Here the sensors are called passive because wthey are only used as receivers. The estimation of the travel time between the passive sensors is possible when the ambient noise sources are randomly distributed, uncorrelated and extend over the whole space, while they are statistically stationary in time [9]. These assumptions, however, are not always satisfied in applications where the noise source distribution is usually spatially limited [11]. In that case, and for a homogeneous background medium, it was shown in [3] that the estimation of the travel time between the two sensors is possible when the ray that connects the two sensors goes through the source region. When the background medium, however, contains random inhomogeneities that cause multiple scattering, the directional diversity of the noisy signals is enhanced and estimation of the travel time is possible for sensor configurations that do not fulfill the above mentioned geometric condition (cf. [5]).

Our starting point is the analysis of J. Garnier and G. Papanicolaou about passive sensor imaging using cross-correlations generated by ambient noise sources [3, 5]. We consider here the imaging problem in a homogeneous background and we analyze the Signal to Noise Ratio (SNR) of the image. Our analysis shows that $\mathrm{SNR} \sim J\sqrt{BT}$, with J being the number of receivers, T the recording time and B the bandwidth. Our numerical results are consistent the theory.

2. SIMULATION SETUP AND MATHEMATICAL MODEL

We consider $u(\mathbf{x}, t)$ the solution of the acoustic wave equation

$$\frac{1}{c_0^2}\frac{\partial^2 u(\mathbf{x},t)}{\partial t^2} - \Delta u(\mathbf{x},t) = n(\mathbf{x},t), \qquad (1)$$

in two dimensions, $\mathbf{x} = (x, z)$, in a medium with homogeneous propagation speed c_0.

We solve the acoustic wave equation with the software Montjoie (*https://gforge.inria.fr/projects/montjoie*) using mixed spectral finite elements [14] of 7th order in space and a finite difference discretization of 4th order in time. We simulate wave propagation in an unbounded environment by surrounding the computational domain with a perfectly matched absorbing layer (PML).

In (1), $n(\mathbf{x}, t)$ models the noise sources. It is a zero mean stationary (in time) random process with correlation function,

$$E\{n(\mathbf{x}_1, t_1)n(\mathbf{x}_2, t_2)\} = \mathbb{F}(t_1 - t_2)K(\mathbf{x}_1)\delta(\mathbf{x}_1 - \mathbf{x}_2).$$

The process n is delta-correlated in space and K characterizes the spatial support of the sources. The time distribution of the noise sources is characterized by the correlation function $\mathbb{F}(t_2 - t_1)$, which in our numerical simulations is given by

$$\mathbb{F}(t) = \int F(\tau)F(t+\tau)d\tau, \quad (2)$$

$$F(t) = \mathrm{sinc}(Bt)\cos(2\pi f_0 t)\exp(-t^2/(2C_t^2)). \quad (3)$$

Here C_t is the correlation length in time, B the bandwidth, and f_0 the central frequency of the sources.

3. DISCRETE WAVE CROSS-CORRELATION

Let $(u(\mathbf{x}_1)_n)_{0\le n<N}$ and $(u(\mathbf{x}_2)_n)_{0\le n<N}$ denote the time-dependant wave fields recorded by two sensors at $\mathbf{x}_1$ and $\mathbf{x}_2$ and at discrete time $t_n = n\delta_t$, for $0 \le n < N$. Their cross-correlation function over the time interval $[-T, T]$, with $T = N\delta_t$, and with time lag $\tau = \nu\delta_t$ is given by

$$C_T(\tau, \mathbf{x}_1, \mathbf{x}_2) = \frac{1}{N}\sum_{n=0}^{N-1-\nu} u(\mathbf{x}_1)_n u(\mathbf{x}_2)_{n+\nu}. \quad (4)$$

Implementing directly (4) in a numerical code is quite easy, but execution time is in $O(N^2)$. Since this formula is close to a discrete convolution formula, we wish to use the Discrete Fourier Transform (DFT) as defined in the GNU Scientific Library [15]. In this case, we extend the wave fields $(u(\mathbf{x})_n)_{0\le n<N}$, for $\mathbf{x} = \{\mathbf{x}_1, \mathbf{x}_2\}$, to $(\tilde{u}(\mathbf{x})_n)_{0\le n<2N}$ defined as

$$\tilde{u}(\mathbf{x})_n = \begin{cases} u_{n-N}, & n \ge N, \\ 0, & \text{otherwise.} \end{cases} \quad (5)$$

We can rewrite the cross-correlation function (4) as, (for the second index we take the remaining in $\{0, \dots, 2N-1\}$ *modulo* $2N$),

$$C_T(\mathbf{x}_1, \mathbf{x}_2)_{N+\nu} = \frac{1}{N}\sum_{n=0}^{2N-1} \tilde{u}(\mathbf{x}_1)_n\, \tilde{u}(\mathbf{x}_2)_{n+\nu}, \quad (6)$$

for $-N \le \nu < N$.

We recall here the DFT,

$$\mathcal{F}(u)_k = \sum_{n=0}^{2N-1} u_n \exp\left(-2\imath\pi\frac{kn}{2N}\right). \quad (7)$$

Proposition 3.1. *The following relation holds,*

$$\mathcal{F}(C_T(\mathbf{x}_1, \mathbf{x}_2))_k = \frac{(-1)^k}{N}\mathcal{F}(\tilde{u}(\mathbf{x}_1))_{-k}\,\mathcal{F}(\tilde{u}(\mathbf{x}_2))_k\,. \quad (8)$$

Relation (8) allows us to compute $C_T(\mathbf{x}_1, \mathbf{x}_2)$ in $O(N)$ steps. Moreover, since the recorded wave fields are real valued, we can rewrite this relation as

$$\mathcal{F}(C_T(\mathbf{x}_1, \mathbf{x}_2))_k = \frac{(-1)^k}{N}\overline{\mathcal{F}(\tilde{u}(\mathbf{x}_1))_k}\mathcal{F}(\tilde{u}(\mathbf{x}_2))_k\,. \quad (9)$$

Computing relation (9) is also in $O(N)$, and has its own interest from a computational point of view.

4. MIGRATION IMAGING

We shall assume that the noise sources are spatially localized and the sensors $(\mathbf{x}_j)_{1\le j\le J}$ are located between the sources and the reflectors. More precisely, rays going through reflectors and sensors reach into the source region, and the sensors are between the reflectors and the sources along these rays. We call this the daylight configuration. We use terminology from analogous situations in photography but it should be kept in mind that imaging is coherent here, which means that the recorded signals are time-resolved amplitudes and not just intensities.

Stationary phase analysis (cf. [3]) shows that the cross-correlation between two sensors $\mathbf{x}_i$ and $\mathbf{x}_j$ is expected to have two peaks: one at the travel time between the two sensors and another one at the sum of the travel times between the sensors and the scatterer. To keep only the interesting peak that concerns the scatterer, the image at a search point $\mathbf{z}$ is computed using the following daylight imaging functional (cf. [3]),

$$\mathcal{I}^{\mathrm{D}}(\mathbf{z}) = 2\sum_{j,l=1}^{J} C_{T,\text{coda}}^{\text{sym}}(\tau(\mathbf{z}, \mathbf{x}_l) + \tau(\mathbf{z}, \mathbf{x}_j), \mathbf{x}_j, \mathbf{x}_l), \quad (10)$$

where $\tau(\mathbf{z}, \mathbf{x}_l)$ is the travel time between $\mathbf{x}_l$ and $\mathbf{z}$:

$$\tau(\mathbf{z}, \mathbf{x}_l) = \frac{|\mathbf{z} - \mathbf{x}_l|}{c_0}, \quad (11)$$

and

$$\begin{aligned} C_{T,\text{coda}}^{\text{sym}}(\tau, \mathbf{x}_j, \mathbf{x}_l) = \big(&C_T(\tau, \mathbf{x}_j, \mathbf{x}_l) \\ &+ C_T(-\tau, \mathbf{x}_j, \mathbf{x}_l)\big)1_{[\tau(\mathbf{x}_j,\mathbf{x}_l),+\infty]}. \end{aligned} \quad (12)$$

If we consider that the scatterer is far enough from the receivers, then we can simplify formula (10). The precise statement is the following:

Proposition 4.1. *The migration imaging functional with daylight illumination is given by*

$$\mathcal{I}^{\mathrm{D}}(\mathbf{z}) = 2\sum_{j,l=1}^{J} C_T(\tau(\mathbf{z}, \mathbf{x}_l) + \tau(\mathbf{z}, \mathbf{x}_j), \mathbf{x}_j, \mathbf{x}_l) \quad (13)$$

5. NUMERICAL SIMULATIONS

We study the acoustic wave propagation on the rectangle $[0, 50\lambda]\times[-15\lambda, 15\lambda]$, with a reflector located in $[44\lambda, 46\lambda]\times[-\lambda, \lambda]$. The random distribution of sources has support on the rectangle $[0, 4\lambda] \times [-15\lambda, 15\lambda]$ (gray region on Figure 1), and we record the solution u of the wave equation at $J = 61$ sensors located at $\mathbf{x}_j = (5\lambda, (j-31)\lambda/2)$, for $1 \le j \le 61$. Length is scaled by the reference wavelength $\lambda = 10\,\mathrm{km}$. The reflector is modeled as a soft acoustic scatterer, *i.e.*, $u = 0$ on the boundary of the reflector.

Figure 1: Geometry of the passive sensor imaging problem for a daylight illumination.

In our simulations we consider that the wave speed is $c_0 = 3\,\mathrm{km\,s^{-1}}$. To model the noise sources we use (3) with $f_0 = 0.3\,\mathrm{Hz}$, $C_t = 2.5\mathrm{s}$ and $B = 0.3\,\mathrm{Hz}$.

Using the daylight imaging functional (13) we compute the image near the scatterer. We show the results on figure 2 Observe that we can recover the location of the scatterer. Moreover, the signal to noise ratio of the image is very good, *i.e.*, we only have one maximum at the correct scatterer location and the noise level is low. The question that naturally arises is "Under what conditions do we obtain such a good image?" or in other words "What are the parameters that control the quality of the image, and how?" The answer to this question can be given by the resolution and the SNR analysis of the imaging functional.

6. RESOLUTION AND SNR ANALYSIS

The resolution analysis of the daylight imaging functional is carried out in [4] when there is a point reflector at $\mathbf{z}_\mathrm{r}$. The cross range resolution for a linear sensor array with aperture a is given by $\lambda_0 L_\mathrm{r}/a$. Here L_r is the distance between the sensor array and the reflector and λ_0 is the wavelength corresponding to the central frequency. The range resolution for broadband noise sources is equal to c_0/B where B is the bandwidth of the noise sources. The peak of the imaging functional is obtained at $\mathbf{z} = \mathbf{z}_\mathrm{r}$. It is independent of T and the peak amplitude is proportional to J^2 in terms of the number of receivers J and proportional to $\int \hat{\mathbb{F}}(\omega) d\omega$ in terms of the power spectral density. Moreover, we have the following results (cf. [3], [16]):

1. The expectation of the empirical cross correlation C_T (with respect to the distribution of the sources) is independent of T:

$$\langle C_T(\tau, \mathbf{x}_1, \mathbf{x}_2)\rangle = C^{(1)}(\tau, \mathbf{x}_1, \mathbf{x}_2),$$

where the statistical cross correlation $C^{(1)}$ is given by

$$\begin{aligned} C^{(1)}(\tau, \mathbf{x}_1, \mathbf{x}_2) &= \frac{1}{2\pi}\int \hat{D}(\omega, \mathbf{x}_1, \mathbf{x}_2)\hat{\mathbb{F}}(\omega) e^{-i\omega\tau} d\omega, \\ \hat{D}(\omega, \mathbf{x}_1, \mathbf{x}_2) &= \int \overline{\hat{G}(\omega, \mathbf{x}_1, \mathbf{y})}\hat{G}(\omega, \mathbf{x}_2, \mathbf{y}) K(\mathbf{y}) d\mathbf{y}, \end{aligned}$$

and $\hat{G}(\omega, \mathbf{x}, \mathbf{y})$ is the time-harmonic Green's function (*i.e.* the Fourier transform of $G(t, \mathbf{x}, \mathbf{y})$).

2. The empirical cross correlation C_T is a self-averaging quantity:

$$C_T(\tau, \mathbf{x}_1, \mathbf{x}_2) \overset{T\to\infty}{\longrightarrow} C^{(1)}(\tau, \mathbf{x}_1, \mathbf{x}_2),$$

in probability with respect to the distribution of the sources.

3. The covariance of the empirical cross correlation is:

$$\begin{aligned} &\mathrm{Cov}\big(C_T(\tau, \mathbf{x}_1, \mathbf{x}_2), C_T(\tau', \mathbf{x}_3, \mathbf{x}_4)\big) = \frac{1}{2\pi T} \\ &\bigg(\int \hat{D}(\omega, \mathbf{x}_1, \mathbf{x}_3)\overline{\hat{D}(\omega, \mathbf{x}_2, \mathbf{x}_4)}\hat{\mathbb{F}}(\omega)^2 e^{-i\omega(\tau'-\tau)} d\omega \\ &+ \int \hat{D}(\omega, \mathbf{x}_1, \mathbf{x}_4)\overline{\hat{D}(\omega, \mathbf{x}_2, \mathbf{x}_3)}\hat{\mathbb{F}}(\omega)^2 e^{-i\omega(\tau'+\tau)} d\omega\bigg), \end{aligned}$$

when $BT \gg 1$ (here B is the bandwidth of the noise sources, *i.e.* of the correlation function $\mathbb{F}$).

In [16] we consider the behavior of the variance of the imaging functionals $\mathcal{I}^\mathrm{D}$. This means that we study the fluctuations of the imaging functionals when the integration time T is not long enough to ensure the validity of the self-averaging relation $C_T = C^{(1)}$. In this case, we show that the signal to noise ratio of the daylight imaging functional

$$\mathrm{SNR}^\mathrm{D} = \frac{\big\langle \mathcal{I}^\mathrm{D}(\mathbf{z}_\mathrm{r})\big\rangle}{\mathrm{Var}\big(\mathcal{I}^\mathrm{D}(\mathbf{z})\big)^{1/2}} \tag{14}$$

is proportional to

$$\mathrm{SNR}^\mathrm{D} \sim J\sqrt{BT} \tag{15}$$

From the numerical point of view we compute the SNR of the image as follows. Let $\overline{\mathcal{I}^\mathrm{D}}(z)$ be the averaged absolute value of the image over a square of size $2\lambda \times 2\lambda$ centered at z. The SNR is computed as

$$\mathrm{SNR} = \frac{\overline{\mathcal{I}^\mathrm{D}}(z^*)}{\max_{z\neq z^*}\overline{\mathcal{I}^\mathrm{D}}(z)} \tag{16}$$

where z^* is the middle point of left edge of scatter, and $z \neq z^*$ means that squares of size $2\lambda \times 2\lambda$ centered at z and z^* do not intersect. We plot the SNR versus number of receivers on figure 3, versus bandwidth on figure 4) and versus time on figure 5. We observe that the numerical results are in very good agreement with the theory.

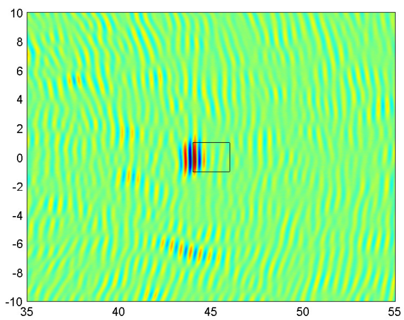

Figure 2: Daylight imaging functional (13) for the homogeneous background medium. Length is in wavelength λ.

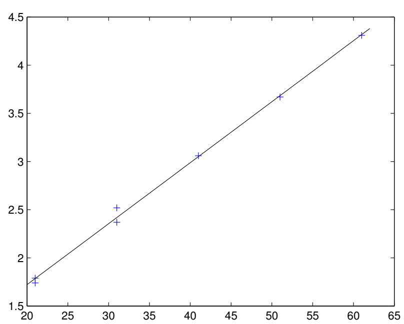

Figure 3: Plot of SNR versus number of receivers

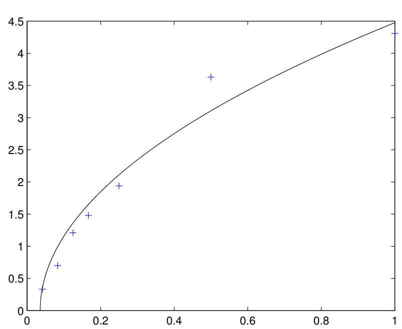

Figure 4: Plot of SNR versus B/f_0

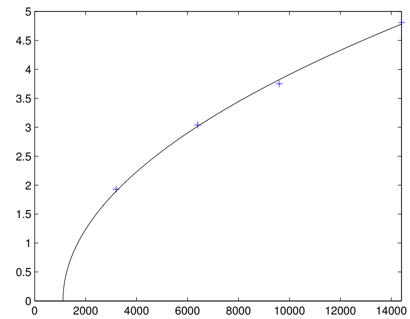

Figure 5: Plot of SNR versus number of time

Acknowledgments

This work was partially supported by the European Research Council Starting Grant, GA 239959 and the FP7-REGPOT-2009-1 project "Archimedes Center for Modeling, Analysis and Computation".

7. REFERENCES

[1] R.L. Weaver and O.I. Lobkis "Ultrasonics without a source: thermal fluctuation correlations at MHz frequencies", Phys. Rev. Lett., Vol. 87 (13), 134301, 2001.

[2] C. Bardos, J. Garnier and G. Papanicolaou, "Identification of Green's functions singularities by cross-correlation of noisy signals", Inverse Problems, 24, 015011, 2008.

[3] J. Garnier and G. Papanicolaou, "Passive sensor imaging using cross correlations of noisy signals in a scattering medium", SIAM J. Imaging Sciences, Vol. 2, pp. 396–437, 2009.

[4] J. Garnier and G. Papanicolaou, "Resolution analysis for imaging with noise", Inverse Problems, Vol. 26, 074001, 2010.

[5] J. Garnier and G. Papanicolaou, "Resolution enhancement from scattering in passive sensor Imaging with Cross Correlations", preprint, 2010.

[6] Y. Colin de Verdière, "Semiclassical analysis and passive imaging", Nonlinearity, Vol. 22, pp. R45–R75, 2009.

[7] K. Wapenaar and J. Fokkema, "Green's function representations for seismic interferometry", Geophysics, Vol. 71, pp. SI33–SI46, 2006.

[8] R. Snieder, “Extracting the Green’s function from the correlation of coda waves: A derivation based on stationary phase”, Phys. Rev. E, Vol. 69, 046610, 2004.

[9] P. Roux, K. G. Sabra, W. A. Kuperman, and A. Roux, “Ambient noise cross correlation in free space: Theoretical approach”, J. Acoust. Soc. Am., Vol. 117, pp. 79–84, 2005.

[10] K. G. Sabra, P. Gerstoft, P. Roux, and W. Kuperman, “Surface wave tomography from microseisms in Southern California”, Geophys. Res. Lett., Vol. 32, L14311, 2005.

[11] L. Stehly, M. Campillo, and N. M. Shapiro, “A study of the seismic noise from its long-range correlation properties”, Geophys. Res. Lett., Vol. 111, B10306, 2006.

[12] L. Borcea, G. Papanicolaou and C. Tsogka, “Interferometric array imaging in clutter”, Inverse Problems, vol 21, pp. 1419-1460, 2005.

[13] L. Borcea, G. Papanicolaou and C. Tsogka, “Adaptive interferometric imaging in clutter and optimal illumination”, Inverse Problems, vol. 22, pp. 1405-1436, 2006.

[14] G. Cohen, “Higher-order numerical methods for transient wave equations”, Springer-Verlag, 2002.

[15] M. Galassi, J. Davies, J. Theiler, B. Gough, G. Jungman, M. Booth and F. Rossi, “GNU Scientific Library Reference Manual”, Revised Second Edition (v1.8), Network Theory Ltd, 2006.

[16] J. Garnier, G. Papanicolaou, A. Semin and C. Tsogka, “Signal to Noise Ratio estimation in passive correlation based imaging”, *in preparation*